Concrete structures under combined stresses: a review of canadian research

Autor(en): **Dilger, Walter H. / Jordaan, Ian J.**

Objekttyp: **Article**

Zeitschrift: **IABSE reports of the working commissions = Rapports des commissions de travail AIPC = IVBH Berichte der Arbeitskommissionen**

Band (Jahr): **19 (1974)**

PDF erstellt am: **21.09.2024**

Persistenter Link: https://doi.org/10.5169/seals-17509

IABSE
AIPC
IVBH

SEMINAR on:
«CONCRETE STRUCTURES SUBJECTED TO TRIAXIAL STRESSES»
17th-19th MAY, 1974 - ISMES - BERGAMO (ITALY)

Concrete structures under combined stresses: a review of canadian research

Betontragwerke unter mehrachsiger Beanspruchung: ein Überblick über Kanadische Forschungsarbeiten

Structures en béton sous contraints triaxiales: vue d'ensemble des recherches conduites au Canada

Walter H. DILGER and Ian J. JORDAAN - Associate Professor
Department of Civil Engineering - The University of Calgary
Calgary, Alberta - Canada

Summary :
Research in Canada into the behaviour of concrete structures under three-dimensional stresses is reviewed. Studies involving the response of materials and structural components include comprehensive investigations into confined concrete under static loading; methods of confinement include lateral binders, lateral prestressing and steel pipes. Dynamic loading of concrete which is restrained laterally with binders has also been studied extensively. Research into the creep, strength and fatigue of concrete under multiaxial stresses is reported. The analysis of structures under three-dimensional stresses includes a comparison of the approximate space frame analysis with coarse and fine mesh 3 D finite element analysis when applied to an arch dam. Lastly, results of photoelastic studies applied to a dam and to conduits are summarized.

Zusammenfassung :
Es wird über Kanadische Forschungsarbeiten über das Verhalten von Betontragwerken unter mehrachsiger Beanspruchung berichtet. Untersuchungen über das statische und dynamische Verhalten der Baustoffe und Bauglieder wurden vor allem an Beton durchgeführt, der durch Querbewehrung, Quervorspannung oder Stahlrohre umschnürt war. Zudem wird das Verhalten des Betons unter Kriech- und Ermüdungsbelastung diskutiert.
Als Beispiel für die Berechnung von Bauwerken unter dreiachsiger Beanspruchung wird ein Staudamm als räumliches Stabtragwerk und mit Hilfe eines groben und feinen Rasters von finiten Elementen berechnet und die Ergebnisse werden verglichen. Zum Schluß werden die Resultate von photoelastischen Untersuchungen an einem Staudamm und an Druckrohrleitungen zusammengefaßt.

Résumé :
Vue d'ensemble des recherches conduites au Canada sur le comportement des structures en béton soumises à un état triaxial de contraintes. Des études sur la réponse des matériaux

et des éléments structuraux comprennent des recherches poussées sur le béton fretté soumis à des charges statiques. Le frettage est assuré par des cadres, une précontrainte transversale, l'enveloppement dans des tubes en acier. Le chargement dynamique du béton fretté par des cadres a également été étudié de facon intensive. La recherche sur le fluage, la résistance et la fatigue du béton sous contraintes pluriaxiales est présentée. Le calcul de structures sous contraintes triaxiales comprend une comparaison du calcul approché à l'aide d'un portique spatial et du calcul par la mèthode des éléments finis (maillage spatial grossier et fin) pour un barrage-voûte. Pour finir, des résultats d'études de photoelasticité sur un barrage et des conduites sont résumés.

1. Introduction

Most concrete structures are subjected to multiaxial stresses but for only very few is the multiaxial state of stress analyzed and considered in design. In many cases one or two stress components are so small that they can be neglected; in others the stress components not considered in the analysis are of significant magnitude but are beneficial so that neglecting them does no harm to the structure. Then there are cases where the multiaxial state of stress is expressed indirectly in empirical design equations and is therefore incorporated in the design without being especially mentioned. As an example of the latter case the shear design of flat slabs may be mentioned.

In addition to those structures requiring three-dimensional stress analysis, there are structural elements such as beams and columns which are idealised in the theory of elasticity as one-dimensional elements in a skeletal frame analysis. In these mem - bers a triaxial state of stress is introduced by the lateral confinement of the concrete. The beneficial effect of the confinement is normally not expressed in design codes because it does not noticeably affect the strength of the member. But with a general trend towards limit design (plastic design) for reinforced concrete structures the increased ductility resulting from the confinement is of paramount importance. Reinforcement confining the concrete in the directions perpendicular to the axis of compression produces a ductile material out of an otherwise brittle (unconfined) material. Besides the above-mentioned cases there are concrete structures, particularly massive ones such as dams and prestressed concrete pressure vessels the design of which requires complete knowledge of all the components of stress. The analysis of these structures requires highly sophisticated analytical and / or experimental techniques which are generally dealt with by specialists.

Recent research work in Canady concerned with three-dimensional stresses in concrete structures can be divided in two categories :

a) Research involving the response of materials and structural components.

b) Methods of analysis.

The response of concrete and structural components to multiaxial stresses has been investigated chiefly at the Universities of Waterloo and Calgary. The research has included experiments under static, dynamic, fatigue and sustained loading conditions. One of the main purposes of the experimental research was to find the response of confined concrete to axial load. The confinement was either produced by lateral binders (non-prestressed and prestressed) or by steel pipes. The results obtained from prism tests were found to provide accurate information to predict the ductility and for stability of reinforced or prestressed members subjected to axial load and / or bending moments.

Creep deformation under sustained multiaxial loading was investigated and reasonable assumptions for the creep analysis in mass concrete structures were suggested. Failure under triaxial stresses is a complex problem, with concrete changing gradually from a brittle to a ductile material with increasing volumetric (compressive) stress. This observation led to a recent study on the fatigue behavior of concrete under combined stresses at The University of Calgary.

Methods of analysis have been concerned with the three-dimensional finite element method. Analytical research on this topic is reported from The University of Calgary. Finite element programs have been developed to analyze concrete arch dams and other massive concrete structures. The analyses were in all cases based on linear elastic material properties.

2. Research on laterally confined concrete

2.1. General

The following are the chief practical means of confining concrete laterally : (1) to provide binders (2) to wrap the member with prestressed wires and (3) to encase the concrete in a steel tube. The first method is the most common. In a structural component binders support the longitudinal reinforcement during pouring of the concrete, prevent the longitudinal bars from buckling, provide shear reinforcement and confine the concrete in the core. Two extensive studies have been concerned with the effect of lateral reinforcement on the strength and behavior of confined concrete, one under static load (1) (2), the other under dynamic load, more specifically under various rates of deformation (3) (4) (5).

2.2. Confined concrete under static load

The study by Sargin [1] and Sargin et.al. [2] at the University of Waterloo represents a comprehensive experimental program involving the following test parameters : concrete strength; size, spacing and strength of the lateral reinforcement; strain gradient; thickness of cover and casting position. Sixty three prisms, of dimensions 125 x 125 x 510 mm, were tested, twenty two of which were of plain concrete; 14 specimens were tested under eccentric load. No longitudinal reinforcement was used in any of the specimens. The cylinder strength of the concrete varied between 16.8 N/mm^2 and 37.6 N/mm^2. The lateral reinforcement consisted of 5 mm, 6 mm or 10 mm diameter plain or 6 mm deformed bars, or of 0.6 mm or 0.9 mm thick plain steel sheet invelopes. The steel had yield strengths between 260 and 480 N/mm^2. The specimens were tested to failure by applying 10 to 30 deformation increments after approximately 60 % of the expected maximum load had been reached. Test duration was 30 to 90 minutes.

In the analysis of the test results, laterally reinforced concrete is treated as a composite material consisting of core and cover.

The parameters of an analytical stress-strain relationship, which was found to describe the mechanical properties of plain and confined concrete adequately, were determined

using a regression analysis of the test results. A stress-strain relationship of the following form was proposed by Sargin [1]

$$\sigma = k_3 f'_c \frac{A x + (D - 1) x^2}{1 + (A - 2) x + D x^2} \qquad (1)$$

where $A = E_c \epsilon_o / k_3 f'_c$

$x = \epsilon / \epsilon_o$

f'_c = cylinder strength of plain concrete

ϵ_o = strain corresponding to maximum stress

ϵ = strain at stress σ

k_3 = ratio of maximum stress to cylinder strength

D = parameter mainly affecting the slope of the descending branch

For concentrically loaded plain concrete specimens the following values were found (units in N/mm^2) :

$$E_c = 5975 \sqrt{f'_c}$$
$$k_3 = 1.00$$
$$\epsilon_o = 0.24\ \%$$

and for eccentrically load plain concrete specimens :

$$E_c = 6530 \sqrt{f'_c}$$
$$k_3 = 1.00$$
$$\epsilon_o = 0.30\ \%$$

If variations in k_3 and ϵ_o due to strain gradient are expressed in terms of kd , the position of the neutral axis, a unified set of equations is obtained for both the concentric and eccentric loading with

$$k_{3c} = k_{30} \{1.0 + q'' [0.007 \quad 125/kd + 0.015 \ (1-0.25\ s/b_e)]\} \qquad (2)$$

and

$$\epsilon_{oc} = \epsilon_{oo} \{1.0 + q'' [\ 0.25 \quad \sqrt{125/kd} + 0.154 \ (1-0.7\ s/b_e)]\} \qquad (3)$$

where subscripts c and o refer to the core and plain concrete, respectively and

$$q'' = 12.05\, p''_e\, f''_y \sqrt{f'_c} \qquad (4)$$

p''_e = volumetric ratio of lateral reinforcement
f''_y = yield strength of lateral reinforcement (N/mm^2)
b_e = width of enclosed core (in mm)
s = spacing of ties (in mm)

The parameter D is adequately represented by

$$D = 0.65 - 7.25\, f'_c \times 10^{-3} \qquad (5)$$

The results obtained from Eq. (1) together with the empirical parameters are compared with sthe strength of confined concrete predicted by a formula based on a theoretical analysis using a classical Boussinesq approach. To this end, the following assumptions were made : (1) the material is linear elastic (2) the medium is semi-infinite (3) the lateral confinement acts uniformly along straight lines and (4) the ties yield before or when the concrete reaches its maximum strength. This theoretical analysis resulted in the following equation [1] :

$$k_{3c} = k_{30} + 16.4\, p''_e\, f''_y \left[\log_e (1+R_s^2) - 3 + (3/R_s) \tan^{-1}(R_s) \right] / \pi f'_c R_s \qquad (6)$$

where $R_s = b_e/s$.

Good agreement was observed between the values of k_{3c} determined from the experimentally based empirical formula and Eq. (6) .

Using Eq. (1) and the appropriate parameters allows accurate prediction of the moment-curvature relationship of reinforced and prestressed concrete members (see Fig. 1).

It was concluded in the study that the effect of lateral reinforcement is dependent on the type, spacing, amount and grade of the binders in addition to the quality of the concrete. The spacing was the most important variable. The concrete confined by the reinforcement was improved in ductility and strength but the concrete outside the core is adversely affected.

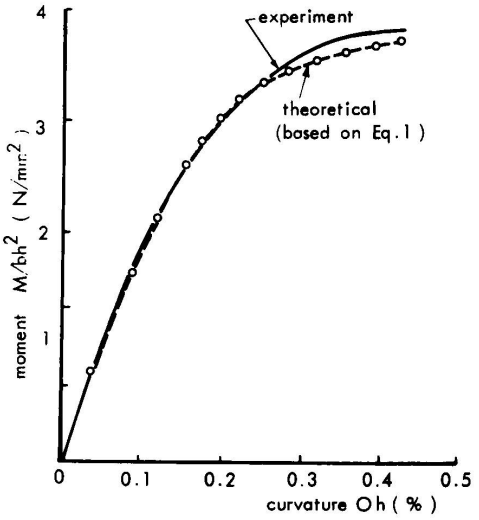

Fig. 1. Moment-curvature diagram for eccentrically loaded column (h = total depth of member)

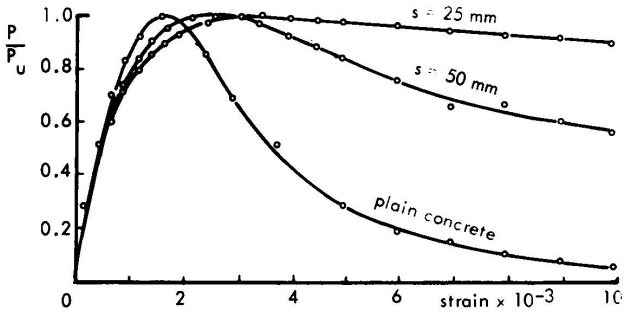

Fig. 2. Stress-strain relationship for plain and confined concrete tested at a strain rate $\dot{\epsilon}$ = 0.32 mm/mm/sec.

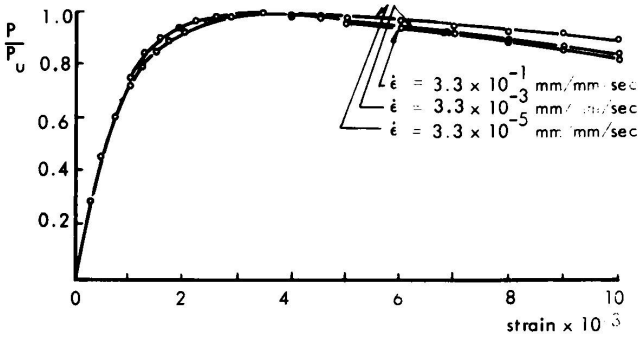

Fig. 3. Stress-strain relationship of confined concrete (spacing of ties 25 mm) subjected to different loading rates

2.3. Confined concrete under dynamic load

The research on transversely reinforced concrete under dynamic load was done during the past five years at the University of Calgary [3] [4] [5]. The main purpose of the research was to investigate the response of confined concrete to various loading rates particularly to extremely high loading rates such as those which occur under catastrophic conditions, for instance in earthquakes and blastwaves. Knowing the response of axially loaded specimens to different strain rates it is possible to establish the response of confined concrete to eccentric loading [6].

The experimental program involved 72 prismatic specimens of dimensions 150 x 150 x 600 mm and the following parameters were investigated : strain rate; type of stirrup (square spirals or discrete ties) and the spacing. The concrete strength was kept constant at about 20 N/mm^2. 24 specimens were not reinforced laterally. The 5 mm plain lateral bars were spaced at 25, 50 or 100 mm and had a yield strength of 248 N/mm^2. The concrete cover was 12.5 mm. The tests were executed in an MTS electrohydraulic closed loop system which allowed a maximum strain rate of 0.33 mm/mm/sec. to be applied to the 600 mm long specimens.

A few typical results are presented in Figs. 2 to 4 : The effect of the transverse reinforcement is shown in Fig. 2. From Fig. 3 it is evident that for confined concrete, the strain rate does not have a significant effect on the shape of the stress-strain diagram. The magnitude of the maximum stress, however, is clearly dependent on the rate of strain as is shown in Fig. 4. From this plot it can also be seen that the effect of the confinement on the strength increase is small compared to the effect of the straining rate.

The results of Ref. (3) have been evaluated by Tadros [6] to incorporate the strain rate in the stress-strain relationship of concrete given by Eq. (1)[1]. To this end the value of the modulus of elasticity E_c was modified according to the following equation:

$$E_c^{(t)} = (1.06 - 0.03 \log_{10} T)\, E_c \qquad (7)$$

where

T = time in minutes to produce a strain of 1000×10^{-6} in the specimen.

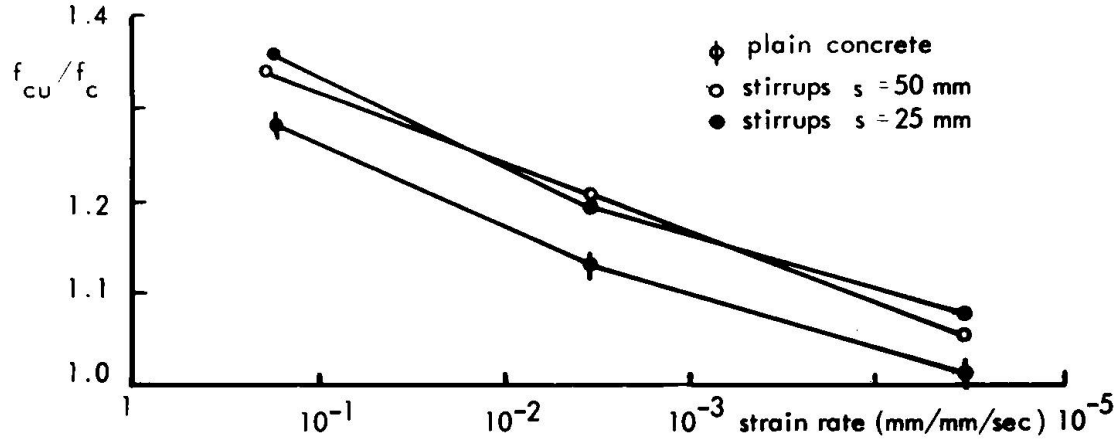

Fig. 4. Relationship between the ratio of failure stress to concrete strength and the strain rate

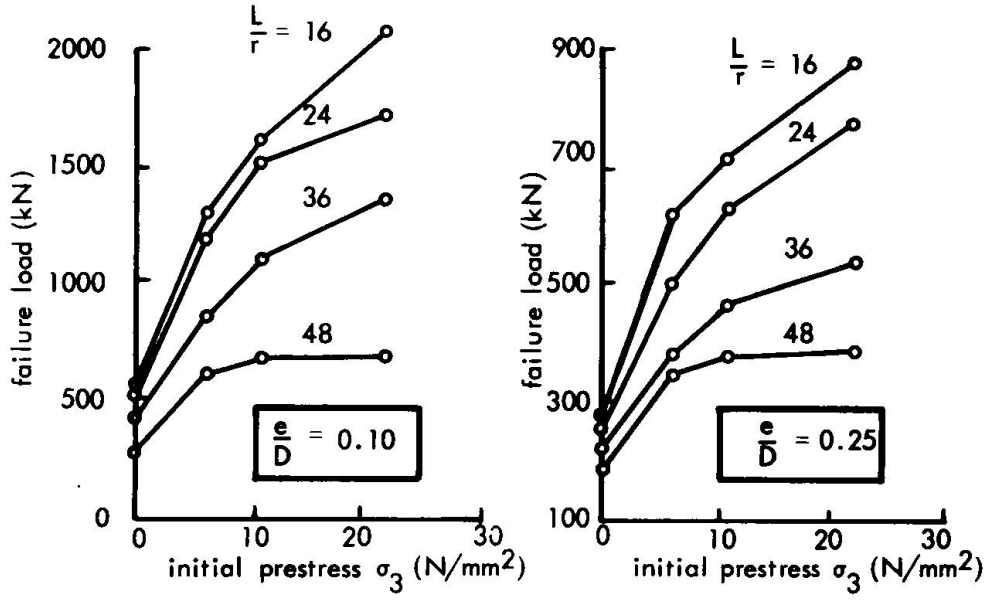

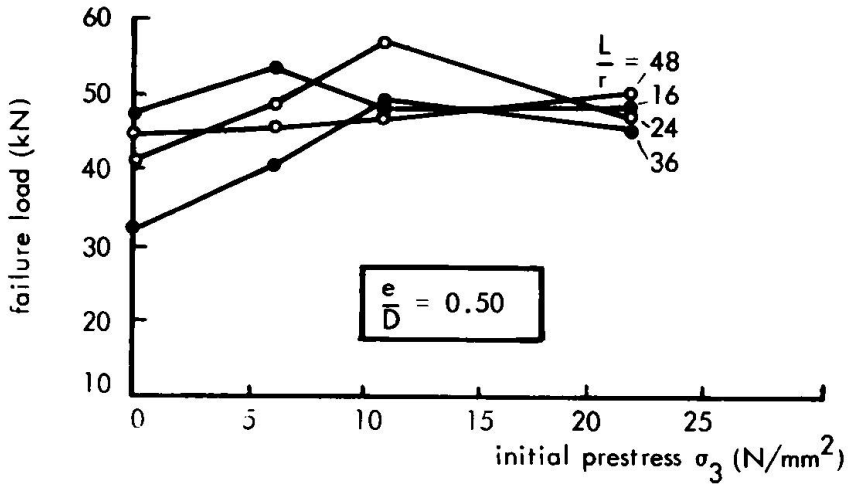

Fig. 5.
Variation of failure load with lateral prestress

The value of ϵ_o had to be modified for different strain rates as follows :

$$\epsilon_o = [0.41 + 0.25 \log_{10} T + 1.14 (6.9 f'_c)^{0.24}] \times 10^{-3} \quad (8)$$

where f'_c is in N/mm^2.

In addition, Tadros [6] introduced the same time factor as in Eq. (7) to take account of the effect of strain rate on concrete strength :

$$k_t = (1.06 - 0.03 \log_{10} T) \quad (9)$$

With these strain-rate dependent parameters good correlation between the experimental and mathematical representation was achieved.

The mathematically formulated stress-strain diagram was used by Tadros to predict the plastic hinge rotation of members subjected to axial load and / or bending moments; again good results were obtained.

2.4. Laterally prestressed short and long columns

Gardner and his co-workers [7] attempted to take advantage of the increased concrete strength under triaxial compression by applying a lateral prestress to concrete columns.

The lateral prestress was applied by wrapping prestressing wires around the column under tension. The lateral prestress was varied between 6.2 and 22.1 N/mm^2 by changing the pitch of the wrappings. Other parameters investigated were the slenderness ratios of the columns and the eccentricity e of the applied load between e/D = 0 and 0.50, where D is the diameter of the column. The results of this investigation can be summarized as follows :

(1) The load carrying capacity of short concrete columns can be increased substantially by prestressing the column by wrapping it with wires under tension.

(2) The failure of the columns is governed by the maximum lateral stress developed in the prestressing wires.

(3) Short columns with small eccentricities ($e/D < 0.5$) will fail by crushing of the concrete and rupture of the wires simultaneously ($\bar{\sigma}_3 = \sigma'_3$) x)

(4) Columns with large eccentricities ($e/D > 0.5$) or large slenderness ratios will fail before the tensile strength of the wires is reached. ($\sigma_3 \leq \bar{\sigma}_3 \leq \sigma'_3$)

(5) In slender column with large eccentricities ($e/D \geq 0.5$) the transverse prestressing has no beneficial effect. A number of characteristic results are depicted in Fig. 5.

(6) The capacity of cylindrical columns with lateral prestressing can be expressed by the following empirical equation :

$$P_{ult} = A'_c \left\{ 0.85 f'_c + 11.6 \left[1 - 0.715 \left(\frac{\bar{\sigma}_3}{f'_c}\right)^{0.2}\right]\left[1.04 - 0.0056 \frac{L}{r} \right] \left(1 - 0.66 \frac{e}{D}\right) \bar{\sigma}_3 \right\}$$

$$\left\{1.042 - 0.0057 \frac{L}{r} \right\} \left\{ 1 - 0.35 \frac{e}{D} \right\} \qquad (10)$$

where $A'_c = \frac{D^2}{4} - 2e\sqrt{\frac{D^2}{4} - e^2} - \frac{D^2}{2} \sin^{-1}\left(\frac{2e}{D}\right)$

for $0 \leq \frac{e}{D} \leq 0.5$

σ_3 = initial stress due to lateral prestressing

σ'_3 = prestress corresponding to the rupture of the wires

$\bar{\sigma}_3$ = final lateral concrete stress at concrete failure lies between initial lateral prestress σ_3 and the value corresponding to the tensile strength of the wires, σ'_3

L = length of column

r = radius of gyration

e = eccentricity

D = diameter of concrete column

---

x) Symbols defined below

2.5. Concrete filled pipe columns

A comprehensive research program on concrete filled steel pipes has been carried out by Gardner and his co-workers [8] [9] [10]. The purpose of this research program was to improve the relevant ACI (American Concrete Institute) and NBC (National Building Code of Canada) design equations, and to find out whether the steel pipe provided lateral restraint to the concrete so that use could be made of the triaxial state of stress in the concrete core.

It was found that the confinement of the concrete by the steel tube does not exist in the initial stages of loading because of the larger Poisson's ratio of steel. In the later stages, particularly towards failure, the lateral deformations of the concrete catch up and hoop stresses in the steel develop which means that the cylindrical steel shell is under a biaxial state of stress resulting from the axial stress $\sigma_{s\ell}$ and the tangential stress σ_t. Assuming that the steel is in a condition of yield when the concrete fails, two extreme bounds are estimated assuming either $\sigma_{s\ell}$ or σ_t' equal σ_y, the yield stress. With $\sigma_{s\ell} = \sigma_y$ (i.e. $\sigma_t = 0$) the capacity of a short column is

$$P_1 = A_c f'_c + A_s \sigma_y \qquad (11)$$

where A_c und A_s are the concrete and steel areas, respectively.

If the steel exerts a circum ferential stress $\sigma_t = \sigma_y$ (i.e. $\sigma_{s\ell} = 0$), the column capacity is

$$P_2 = A_c f'_c + \frac{k}{2} A_s \sigma_y \qquad (12)$$

where k is an empirical factor expressing the effect of lateral stresses on the strength of the concrete, normally k = 4.

By assuming that the maximum shear stress theory holds, i.e. $\sigma_t + \sigma_{s\ell} = \sigma_y$ the column capacity is

$$P_3 = A_c f'_c + \frac{k}{2} A_s \sigma_t + A_s \sigma_{s\ell} .$$

From the experiments it was found that the steel tube yielded first in longitudinal direction, but at failure the steel had yielded also in the tangential direction.

The capacity of the short columns was best predicted by P_3; P_1 was always much lower and P_2 higher than the experimental values.

For long columns it was found that the tangent modulus approach, normally used to predict the buckling load of steel columns, leads to unsafe results because estimating the tangent modulus from a uniaxial test leads to a higher value than that of a column where the steel is biaxially stressed; the presence of the hoop stress reduces the magnitude of the axial stress at which yield occurs. Near yield the magnitude of the tangent modulus decreases rapidly so that a small hoop stress can result in a large reduction of the tangent modulus.

In reference [8] interaction curves are presented for various axial loads and moments; in addition suggestion for design procedures are given.

3. Multiaxial creep, strength and fatigue behaviour of plain concrete

3.1. Creep of plain concrete

It is necessary in the analysis of structures for the effect of creep to have reasonable assumptions of material behaviour in mathematical form. In steel and other metals it is customary to assume that the response to volumetric stresses is elastic and that creep is entirely deviatoric - in other words that the volume does not change as a result of creep. Early work showed that this assumption is not valid for concrete but several investigations subsequently showed conflicting results. Difficulties in experimentation were encountered because of the very small strains to be measured and because of platen effects at the interface between the concrete and the loading device [11]. It became clear, however, that the Poisson's ratio for creep was between zero and the static elastic value.

The moisture condition of the concrete is a most important variable in considering the axial compliance and it is to be expected that it will influence the lateral compliance as well. For sealed concrete the assumption of a constant Poisson's ratio equal to the static elastic value is reasonable as shown in the strain predictions in Figs. 6 to 8 from the work by Jordaan and Illston [12] [13]. For cases where the concrete is not sealed, a direct method for three-dimensional analysis is discussed in a personal contribution [14] in which the effect of drying on the analysis is outlined. It is shown that, even though it is not exact, the assumption of a constant Poisson's ratio is reasonable even for drying concrete. The complications involved in using a more sophisticated assumption are not justified by the additional accuracy obtained, except perhaps in exceptional cases.

3.2. Strength and fatigue under triaxial stresses

A series of static tests in which strengths and deformations of plain concrete were determined at the University of Western Ontario has been described by Gardner [15]. Twenty eight specimens were tested in a triaxial cell and the results were compared to an approximate theory based on the strength and deformational characteristics of a packing of praticles under triaxial stress. Reasonable agreement was found at lower stresses (less than 80 percent of ultimate); with a modification the theory reduces to the Richart-Brandtzaeg-Brown formula

$$\sigma_{1\,max} = k_3\,\sigma_3 + k_4$$

in which $\sigma_{1\,max}$ = ultimate axial stress on cylinder with lateral confining pressure σ_3 and k_3, k_4 = constants.

An investigation was undertaken at the University of Calgary [16] to determine whether the fatigue life of concrete is dependent on the state of stress of the concrete. Cylindrical specimens were subjected to an constant radial confining pressure and axial fatigue loadings. The 102 mm diameter by 305 mm cylindrical specimens were sealed and the loading age was five weeks.

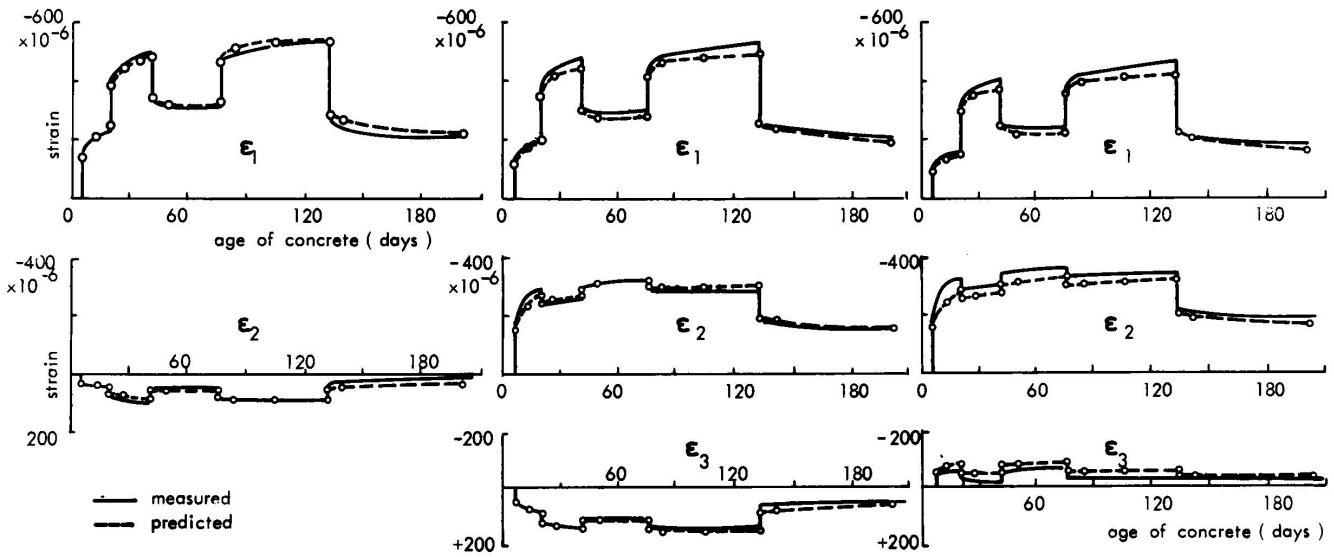

Fig. 6. Strain vs. time plot for uniaxial loading

Fig. 7. Strain vs. time plot for biaxial loading

Fig. 8. Strain vs. time plot for triaxial loading

The tests were performed in a triaxial cell in which volumetric pressure was applied by means of hydraulic fluid while the axial load on the cylinders was applied mechanically by an MTS electrohydraulic loading system.

The static triaxial strengths were determined in static tests at the same confining pressure as the corresponding fatigue test; the minimum stress in the fatigue test was 20% of the static value while maxima of 80 %, 85 % and 90 % were included in the test series. The frequency of load application was in general kept constant at 60 cycles per minute.

Results of the tests are summarised in Table 1; analysis shows that at the 90 % stress level there was no significant effect on the fatigue life, while at the 80 % level a significant improvement resulted from the imposition of lateral confining pressure. The report suggests that the fatigue behaviour is affected by the change in the local state of stress at crack tips, thus suppressing the propagation of cracks. The state of stress is therefore an important variable in the study of fatigue of concrete.

TABLE 1 RESULTS OF FATIGUE TESTS

Lateral pressure, N/mm^2 (psi)	0		6.9 (1,000)			13.8 (2,000)	
Maximum stress level as a proportion of the static strength	0.80	0.90	0.80	0.80	0.90	0.80	0.90
Average number of cycles sustained, N	818	28	90,280 (15,000)xx	1,675 (57,140)+	158	(16,750)x	19.2
Average of $\log_{10}N$	2.71	1.38	4.92 (4.18)	2.90 (4.76)	1.83	(4.19)	1.22

x Five run-out specimens
xx Five run-out specimens
\+ One run-out specimen

4. Analytical and Experimental Analysis of Three Dimensional Concrete Structures

4.1. Three-Dimensional Finite Element Analysis of Concrete Structures

The finite element method is being used more and more extensively in the analysis of three-dimensional structures such as arch dams, or pressure vessels for nuclear power stations. In a paper entitled "Analysis of Arch Dams Using a Space Frame Model" Skjolingstad and Cheung [17] examine the stresses in an arch dam using space frame analogy and compare the results with those obtained from a coarse and fine mesh finite element analysis.

In the analysis the isoparametric hexahedron finite element with 20 nodal points has been used. This element has been proven among other by Skjolingstad [18] to be one of the most accurate and convenient means of analysis for three-dimensional solids. The deflections and stresses for the space frame were obtained utilizing the STRUDL-1 computer program. The doubly curved arch dam of Fig. 9 is used for comparison. Fig. 10 shows the location of the horizontal and vertical members for the space frame analysis and Fig. 11 shows the division of the dam into 32 and 15 elements respectively. From the comparison of the result in Fig. 12 it is evident that the space frame gives in most cases a reasonable estimate of the magnitude of the stresses, which is sufficiently accurate for a preliminary design of a dam. For the final design , however, a fine mesh 3 D finite element analysis is recommended by the authors.

4.2. Photoelastic Analysis

In addition to analytical methods, photoelastic methods to study the three-dimensional behaviour of structures have been used in Canada. A paper by Jones and Mantle [19] on "Three-Dimensional Photoelastic Analysis of a Diamond-Head Buttress Dam" describes a study on a model of the Squaw Rapids Power Development on the Saskatchewan River. The dam (see Fig. 13) was analyzed for water pressure and earth fill at the upstream face and for earth fill from elevation 295 m down at the downstream face. The frozen-stress technique was adopted to obtain an indication

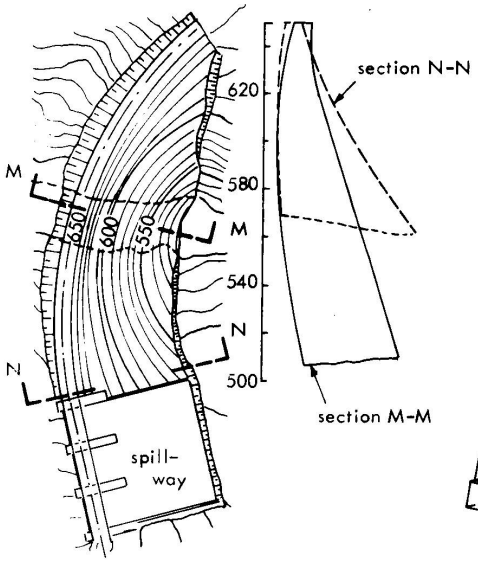

Fig. 9. Plan and cross section of the arch dam used for analysis

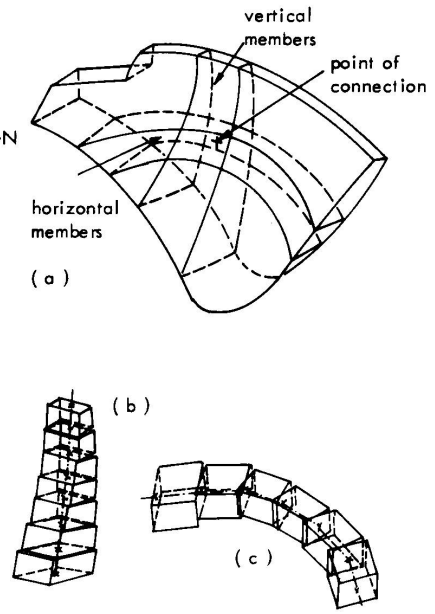

Fig. 10. (a) The arch dam showing the location of (b) typical vertical and (c) typical horizontal members

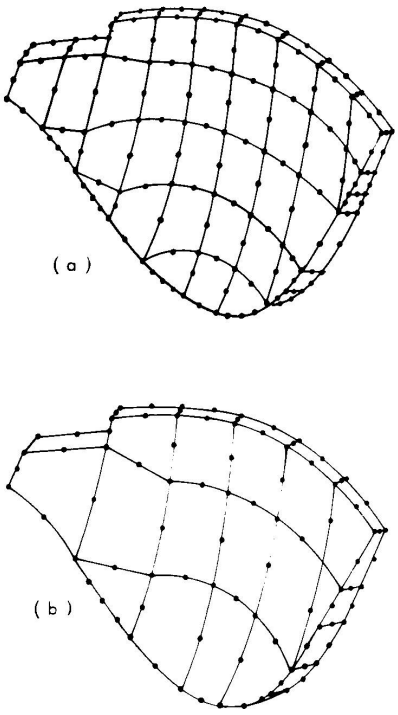

Fig. 11. (a) Fine and (b) coarse finite element mesh

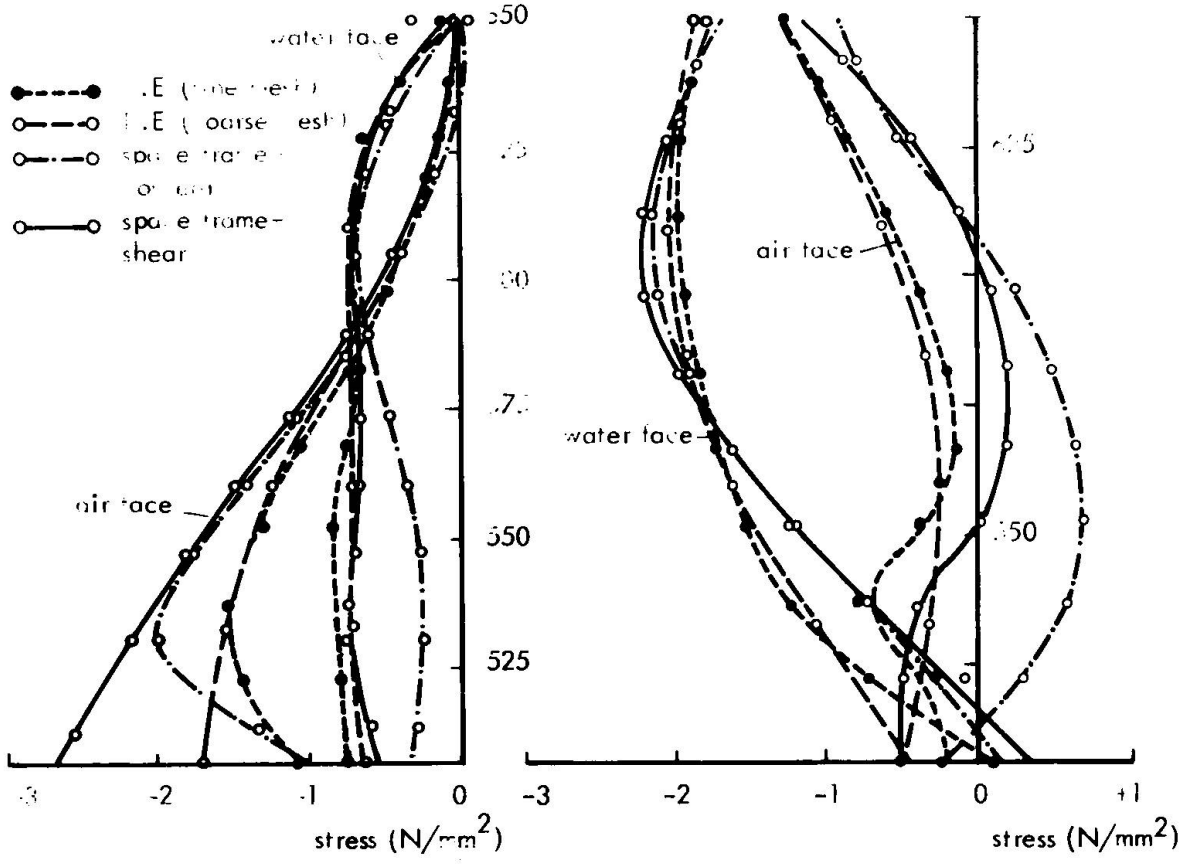

Fig. 12. (a) Vertical stresses at section A and (b) hoop stresses at section A-A

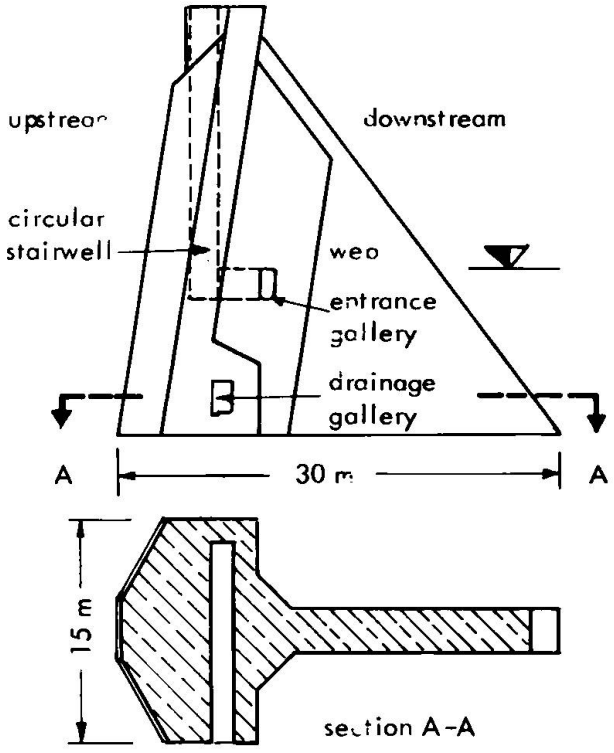

Fig. 13. Unit of buttress - vega dam

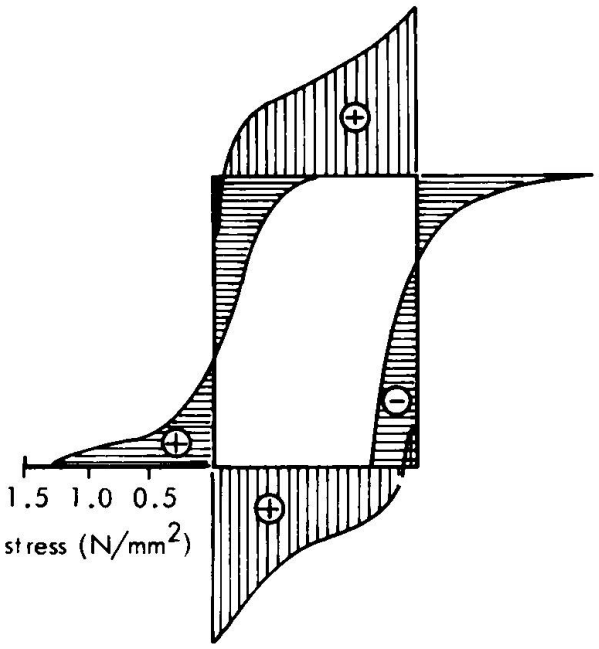

Fig. 14. Tangential stress distribution around gallery

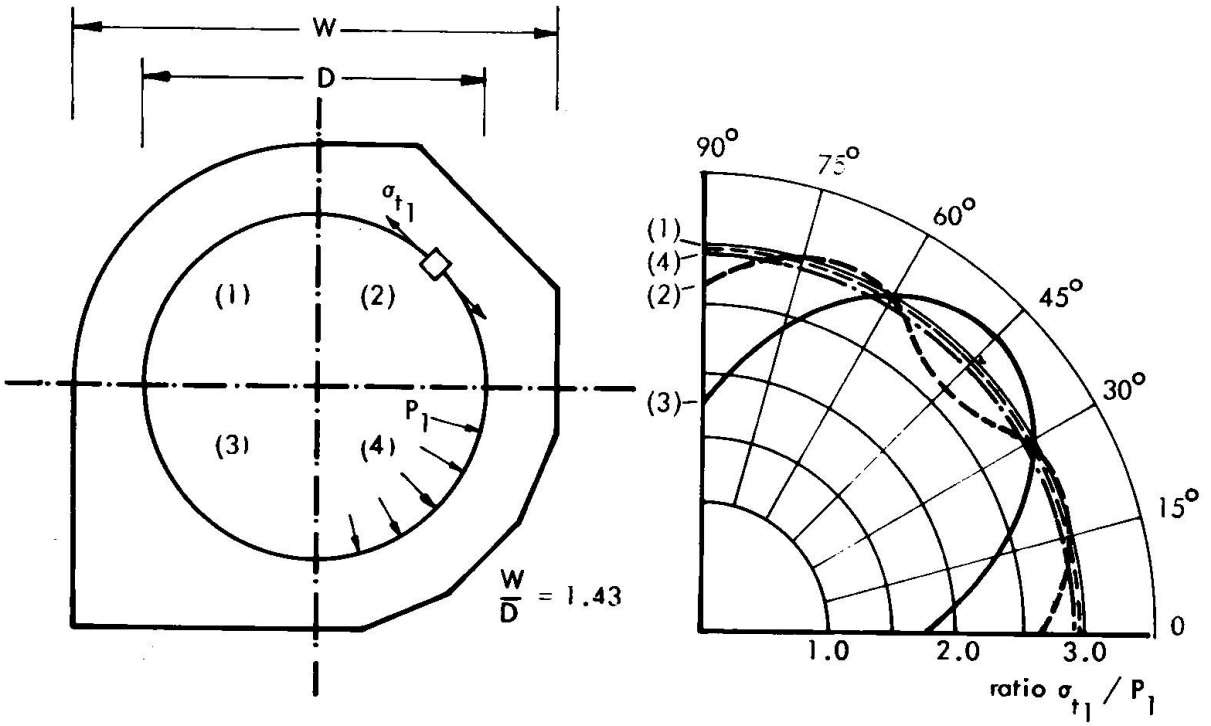

Fig. 15. Cross section and distribution of tangential stress at inside boundary for different cylinders :
(1) Thick cylinder (2) Oktagon (3) Square (4) 16 sided polygon

of the stress that might be expected in the buttresses, especially in the regions of the stairwells and the galleries.

The results of the photoelastic analysis did not show up any extreme stress concentrations and proved the original design to be adequate. The final design of the structure called for reinforcement to be placed around the stairwell and the galleries and for fillets to be provided at the corner of the galleries in order to provide for the high tensile stresses (see Fig. 14).

In another photoelastic study [20] the stresses in conduits with cylindrical internal surfaces and non-cylindrical external boundaries were determined. The external shapes considered were square and polygonal, and curves of stress distributions were presented to make rapid design possible. A typical stress pattern is shown in Fig. 15.

Titres des Figures

Fig. 1 relation moment-courbure d'un poteau chargé excentriquement (h = hauteur totale de l'élément structurel)

Fig. 2 relation contrainte-déformation pour le béton seul et le béton fretté (vitesse de déformation $\dot{\epsilon}$ = 0,32 mm/m/sec.)

Fig. 3 relation contrainte-déformation du béton fretté (espacement des cadres 25 mm) pour plusieurs vitesses de déformation

Fig. 4 relation entre le rapport contrainte ultime / résistance du béton et la vitesse de déformation

Fig. 5 variation de la charge ultime en fonction de la précontrainte transversale

Fig. 6 allongement en fonction de l'age du béton dans le cas du chargement uniaxial

Fig. 7 allongement en fonction de l'age du béton dans le cas du chargement biaxial

Fig. 8 allongement en fonction de l'age du béton dans le cas du chargement triaxial

Fig. 9 vue de dessus et section du barrage-voûte utilisé pour le calcul

Fig. 10 (a) barrage voûte exhibitant la disposition des éléments (b) verticaux et (c) horizontaux typiques

Fig. 11 maillage (a) fin et (b) grossier par les éléments finis

Fig. 12 contraintes (a) verticales et (b) orthoradiales dans la section A-A

Fig. 13 élément caractéristique du barrage

Fig. 14 répartition des contraintes autour de la galerie

Fig. 15 section droite et répartition des contraintes normales le long de la face interne pour differents cylindres

(1) anneau épais
(2) octogone
(3) carré
(4) polygone à 16 cotés

Bildunterschriften

Bild 1 — Momenten-Krümmungs-Diagramm für eine exzentrisch belastete Stütze (h = Gesamthöhe)

Bild 2 — Spannungs-Dehnungs-Diagramm von Beton mit und ohne Umschnürung (Dehngeschwindigkeit ϵ = 0,32 mm/mm/sec)

Bild 3 — Spannungs-Dehnungs-Diagramm von umschnürtem Beton (Bügelabstand 25 mm) unter verschiedenen Dehngeschwindigkeiten

Bild 4 — Beziehung zwischen dem Verhältnis von Bruchspannung und Zylinderdruckfestigkeit und der Dehngeschwindigkeit

Bild 5 — Zusammenhang zwischen Bruchlast und Quervorspannung

Bild 6 — Dehnung als Funktion der Zeit bei einachsiger Belastung

Bild 7 — Dehnung als Funktion der Zeit bei zweiachsiger Belastung

Bild 8 — Dehnung als Funktion der Zeit bei dreiachsiger Belastung

Bild 9 — Grundriß und Querschnitt der untersuchten Bogenstaumauer

Bild 10 — (a) Bogenstaumauer mit der Lage von (b) typischen vertikalen und (c) typischen horizontalen Gliedern

Bild 11 — (a) Feines und (b) grobes Raster der finiten Elemente

Bild 12 — (a) Vertikale und (b) tangentiale Spannungen im Schnitt A-A

Bild 13 — Element der Staumauer

Bild 14 — Spannungsverteilung um die Gallerie

Bild 15 — Querschnitt und Verteilung der Tangentialspannung an der Innenseite verschiedener Zylinder

(1) Dickwandiger Zylinder

(2) Achteck

(3) Quadrat

(4) 16 - seitiges Polygon

References :

(1) Sargin, M.:
"Stress-Strain Relationships for Concrete and the Analysis of Structural Concrete Sections."
Study No. 4, Solid Mechanics Division, University of Waterloo, Waterloo, Ontario, Canada 1971, pp. 167

(2) Sargin, M., S.K. Gosh and V.K. Handa :
"Effects of Lateral Reinforcement upon the Strength and Deformation Properties of Concrete."
Magazine of Concrete Research, Vol. 23, No. 75-76, June-September 1971, pp. 99-110

(3) Kowalczyk, R. and W.H. Dilger:
"Strength and Behaviour of Concrete Under High Strain Rates."
Polish Academy Nauk, Report No. 44, 1971, pp.80

(4) Kowalczyk, R. and W.H. Dilger:
"Ductility of Plain and Reinforced Concrete."
Polish Engineering Archiv, August 1972, pp. 72

(5) Dilger, W.H., R. Kowalczyk and R. Koch:
"Strength and Behaviour of Confined Concrete Subjected to Different Strain Dates."
Submitted for Publication, pp. 18

(6) Tadros, G.S.:
"Plastic Rotation of Reinforced Concrete Members Subjected to Bending, Axial Load and Shear."
Ph.D. Thesis, University of Calgary, 1970, pp.298

(7) Gardner, N.J., R.M. Godse and T.T. Wong:
"Experimental Investigation in the Use of Laterally Prestressed Concrete Columns."
RILEM, International Symposium Buenos Aires, Argentinia, Sept. 1971, pp. 169-193

(8) Gardner, N.J.:
"Design of Pipe Columns."
Transactions of the Engineering Institute of Canada, Vol. 13, No. 3., 4. March 1970, pp. 6

(9) Gardner, N.J. and E.R. Jacobson:
"Structural Behaviour of Concrete Filled Steel Tubes."
ACI Journal, July 1967, pp. 404-414

(10) Gardner, N.J.:
"Use of Spiral Welded Steel Tubes in Pipe Columns."
ACI Journal, November 1968, pp. 937-942

(11) Illston, J.M, I.J.Jordaan and L.J.Parrott:
"The Measurement on Estimation of the Strain in Concrete Under Multiaxial Stress."
The Deformation and the Rupture of Solids subjected to Multiaxial Stresses, RILEM International Symposium, Cannes, 1972, pp. 113-129

(12) Jordaan, I.J. and J.M.Illston:
"The Creep of Sealed Concrete Under Multiaxial Compressive Stress."
Magazine of Concrete Research Vol. 21, No. 69, December 1969

(13) Jordaan, I.J. and J.M. Illston:
"Time-Dependent Strains in Sealed Concrete Under Systems of Variable Multiaxial Stress."
Magazine of Concrete Research Vol. 23, No. 75-76, June-September 1971

(14) Jordaan, I.J.:
"Analysis of Creep in Concrete Structures under General States of Stress."
Personal Contribution, IABSE Seminar on Concrete Structures subjected to Triaxial Stresses, Bergamo, 1974

(15) Gardner, N.J.:
"Triaxial Behaviour of Concrete."
Journal of the American Concrete Institute, Vol. 66, 1969, pp. 136-146

(16) Takhar, S.S., I.J. Jordaan and B.R.Gamble:
"Fatigue of Concrete under Lateral Confining Pressure."
American Concrete Institute Special Publication (in press)

(17) Skjolingstad, L. and Y.K.Cheung:
"Analysis of Arch Dams Using a Space-Frame Model."
Water Power, Febr. 1973

(18) Skjolingstad, L.:
"Three-Dimensional Stress Analysis and Field Problems by the Finite Element Method."
M.Sc.Thesis, The University of Calgary, 1970

(19) Jones, C.R. and J.B.Mantle:
"Three-Dimensional Photoelastic Analysis of a Diamond-Head Buttress Dam."
The Engineering Journal, September 1961,
The Journal of the Engineering Institute of Canada

(20) North, W.P.T. and J.B. Mantle:
"Photoelastic Study of Stresses in Hydrostatically Loaded Cylinders with Noncircular External Boundaries."
Experimental Mechanics, March 1962